Environ Earth Sci
DOI 10.1007/s12665-013-2728-x

ORIGINAL ARTICLE

An investigation of moisture sources and secondary evaporation in Lanzhou, Northwest China

Qian Ma · Mingjun Zhang · Shengjie Wang · Qiong Wang · Wenli Liu · Fei Li · Fenli Chen

Received: 17 January 2013 / Accepted: 9 August 2013

Abstract The purpose of this study is to investigate the atmospheric water cycle in Lanzhou and surrounding areas, a place sensitive to climatic conditions and located in the vertex of the "Monsoon Triangle" of China; this study obtained 243 event-based precipitation samples from four stations in Lanzhou, Yongdeng, Yuzhong and Gaolan for 1 year from April 2011 to March 2012. The seasonal variations of δ^{18}O and d excess indicate that westerly water vapor, local moisture and summer monsoon all have an influence in this region on a large scale. The westerlies play a dominant role. However, the impact of monsoon moisture has a seasonal limitation, mainly during the period from June to early August. On a local scale, the transportation of moisture appears via two routes. The contribution rate of recycling moisture, over the region, is only 3.6 % on average due to the deficiency of water resource in arid and semi-arid land. Additionally, the effect of secondary evaporation has also been discussed, and the results show that relative humidity, temperature and precipitation amount have different impacts on the effect. However, the influence of precipitation amount is not obvious when the rainfall amount is below 10 mm, while the meteorological parameters of relative humidity and temperature play a significant role in that scope.

Keywords Lanzhou · Water cycle · Moisture source · Secondary evaporation · Evapotranspiration

Q. Ma · M. Zhang (✉) · S. Wang · Q. Wang · W. Liu · F. Li · F. Chen
College of Geography and Environmental Science, Northwest Normal University, Lanzhou 730070, China
e-mail: mjzhang2004@163.com

Introduction

Stable isotope is regarded as a diagnostic tool which is utilized in different mediums and widely used in geoscience and environmental studies (Vodila et al. 2011; Kumar et al. 2010; Carroll et al. 2006), using the hydrogen and oxygen isotopes in rivers, lakes and groundwater to investigate the circulation mechanism as well as the surface runoff composition in drainage basins (Zhao et al. 2011), and making use of the isotopic data from speleothems (Lachniet 2008), tree rings (Kress et al. 2010) and ice cores (Steen-Larsen et al. 2011) to reconstruct paleoclimate.

Precipitation is a main input factor in atmospheric water cycle and it contains two natural tracers (^{18}O and ^{2}H) which have strong signals for tracking the trajectories of water vapor. The investigations about changes in moisture sources are popular by using the following two methods. The first method is a model-based study, which relies on the Rayleigh model (Dansgaard 1964). Recently, some scholars have used the model to simulate the variations of δ values in different areas to confirm the water vapor sources (Sengupta and Sarkar 2006; Yamanaka et al. 2007). However, although the model can be used to simulate the evolution of δ values well, it still has its limitations. According to Criss (1999), the deuterium excess (d excess, defined as $d = \delta D - 8\delta^{18}O$; Dansgaard 1964), which is controlled by the relative humidity in moisture source (Pfahl and Wernli 2008) and considered to be the most direct indicator to trace the water vapor source, cannot be effectively predicted by the Rayleigh model. The second approach is to comprehensively analyze the variations of δ^{18}O and d excess for discussing the atmospheric water cycle (Xie et al. 2011). On the other hand, the d excess is not only influenced by the relative humidity in water vapor source, but it has been changed by the effect of evapotranspiration during the movement of air mass and secondary evaporation under the cloud base (Gat 1996). For this reason, the two factors above have to be taken into consideration when the moisture sources have been discussed. Many researchers have investigated the effect of evapotranspiration and sub-cloud evaporation, and accumulate huge theoretical basis (Peng et al. 2007; Liu et al. 2008; Peng et al. 2010; Xu et al. 2011; Froehlich et al. 2008; Gat et al. 1994; Gat and Matsui 1991).

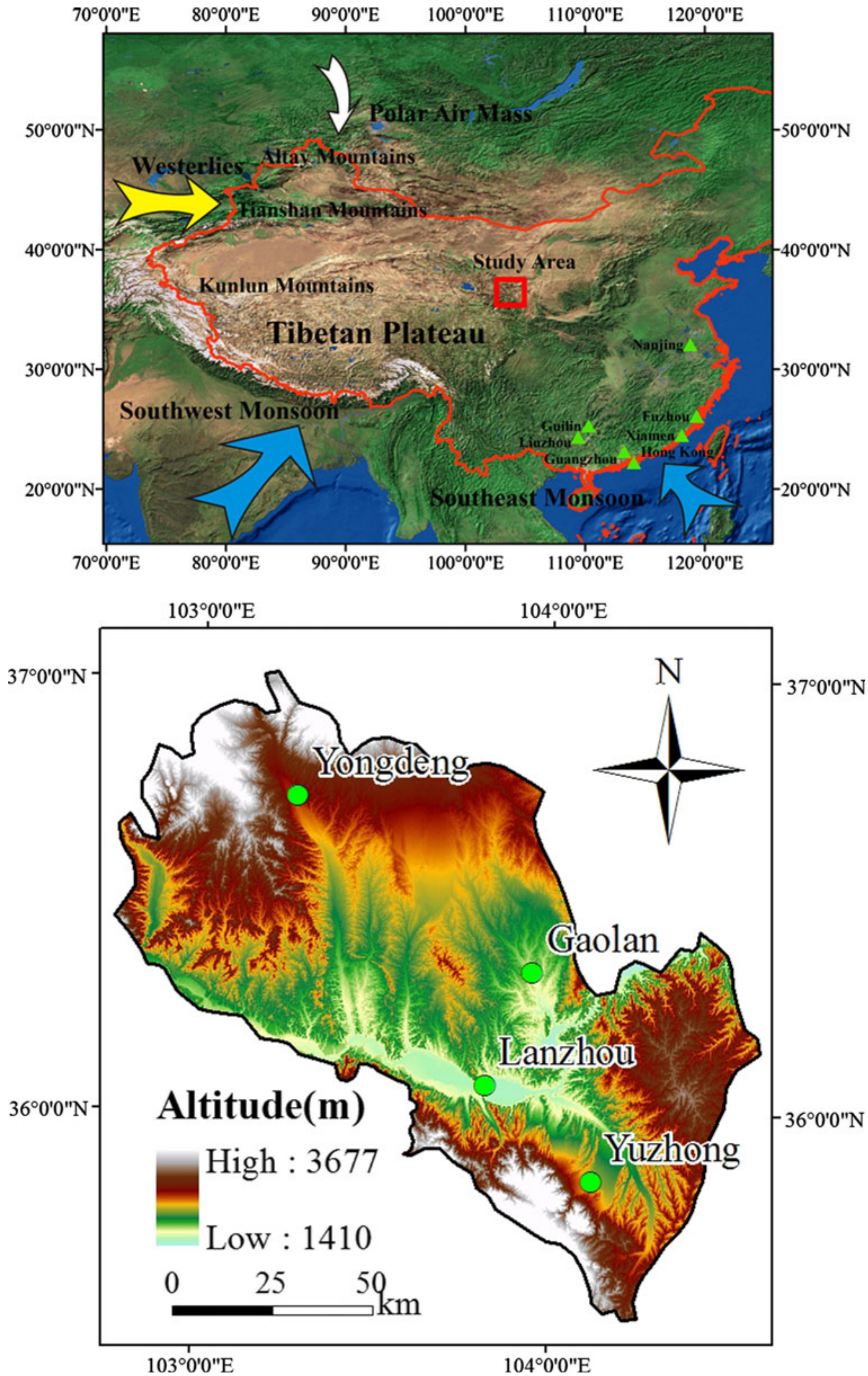

Fig. 1 Map showing the location of study area in China and the distributions of sampling sites. The *arrows* show the major moistures influencing China. The *solid triangles* in the upward map refer to the stations in southeastern China, and the *solid green circles* in the downward map are sampling stations. The *terrain-color reference* shows the variation in altitude within the study area

Monsoon margin (Qian et al. 2009) is closely associated with the concept of global monsoon. Changes in global or Asian monsoon circulation have a great impact on hydrological process in margin of monsoon regions, and play an important role in climatic variability in northern China. Lanzhou and surrounding areas are located in the vertex of the "Monsoon Triangle" of China (Li et al. 1988), a place very susceptible to climatic changes (Qian et al. 2007) and easy-to-occur meteorological and geologic disasters. Due to its unique location, the water cycle mechanism in Lanzhou and surrounding areas is complex. However, related research on this regime is still limited, and the water cycle in Lanzhou needs further investigation. Based on 243 event-based precipitation samples collected in Lanzhou and surrounding areas from April 2011 to March 2012, this paper focuses on the following two problems. The primary one is to determine the water vapor sources influencing the region on different scales and to calculate the contribution rate of evaporation from surface water body through a model, and the second is to explore the existing, impact factors of sub-cloud evaporation.

Study area

The study region of Lanzhou and surrounding areas is in the inland of northwest China (Fig. 1). To its northwestern direction, three mountain ranges which are Altay Mountains, Tianshan Mountains and Kunlun Mountains stretch in that zone, and two low-lying desert basins, Junggar Basin and Tarim Basin, are located between the three mountain ranges. To the southwestern direction, there is the Tibetan Plateau, which is the largest plateau in the world; and to its southeast, there are the monsoon areas of eastern China, which mainly contain plains and hills having a relatively lower elevation.

In western China, there are mainly three air masses influencing the region. Westerlies play a dominant role in northwest China in all seasons, and the polar air mass affects that region mainly in July (Pang et al. 2011). The Tibetan Plateau blocks the southwest monsoon moisture originating from the Indian Ocean in summer. However, still the southwest monsoon moisture climbs the Himalayas and influences the south of the plateau. In winter, the westerly water vapor brings moisture to most of the Tibetan Plateau (Tian et al. 2007). In southeast China, the southeast monsoon moisture gives precipitation to that area during summer.

The study area is located in the intersection of the Tibetan Plateau and monsoon areas in eastern China, near the headwaters of the Yellow (Huanghe) River and far away from oceans. There is low precipitation in the region, which has a mean annual rainfall amount of 293.9 mm in Lanzhou (1981–2010), concentrated from June to September. The mean annual temperature is 10.4 °C in Lanzhou. The hottest month is July with an average temperature of 23.1 °C, while the coldest month is January which has a mean value of −4.5 °C.

In the study area, four stations of Lanzhou, Yongdeng, Gaolan and Yuzhong, evenly distributed from north to south, are chosen for precipitation sampling. The two stations of Yongdeng and Gaolan are located to the north of the Yellow River, and Lanzhou is closer near the river, and Yuzhong is located to the south of the river.

Sample collection and data analysis

In this study, 243 event-based precipitation samples were collected. The samples of the Lanzhou station were collected from the meteorological field in Northwest Normal University, and other samples were taken at the national meteorological stations of Yuzhong, Yongdeng and Gaolan. The detailed information is shown in Table 1. In order to prevent the evaporation of the rain samples, the samples were taken immediately at the end of each event. All of the samples were sealed in 60-mL plastic bottles, and then kept in a refrigerator below 0 °C. The corresponding meteorological parameters, such as temperature, precipitation amount, relative humidity, vapor pressure, wind direction and wind speed, were obtained from the national meteorological stations of Lanzhou, Yuzhong, Yongdeng and Gaolan. Before analysis, the samples were stored at 4 °C in the refrigerator to melt gradually.

All of the samples were measured by a liquid water isotope analyzer DLT-100 [Los Gatos Research (LGR), Inc.] operated in the Laboratory of Isotope Geo-chemistry at the Northwest Normal University. The standards were

Table 1 The detailed information of the sampling sites

Station	Latitude (°N)	Longitude (°E)	Sampling period	Number of samples
Lanzhou	36.07	103.82	April 2011–March 2012	54
Yuzhong	35.85	104.12	April 2011–March 2012	78
Yongdeng	36.73	103.27	April 2011–March 2012	86
Gaolan	36.33	103.95	May 2011–September 2011	25

obtained from LGR Inc., and in the Northwest Normal University, they were calibrated with standard light Antarctic precipitation (SLAP) and Vienna standard mean ocean water (VSMOW). The precision was 0.2 ‰ for δ^{18}O and 1 ‰ for δD, respectively (West et al. 2010).

Results and discussion

Variation of δ^{18}O and local meteoric water lines

The variations of δ^{18}O can reflect the differences of moisture sources and meteorological conditions between different sites (Wu et al. 2010). The values of δ^{18}O varied from −18.2 to 4.7, −19.7 to 3.9 and −17.0 to 4.1 ‰ for Lanzhou, Yuzhong and Yongdeng, respectively. As a result of the relative shorter sampling period at Gaolan which was only sampled from May to September in 2011, the trend of δ^{18}O values, which ranged between −13.1 and 1.4 ‰, is slightly less than the three above. After a comprehensive analysis of the four sites, it is not difficult to find that the range of δ^{18}O values has a similarity to some degree. It indicates that the four stations may have been affected by the same moisture sources on a large scale.

By using all the isotopic data, the monthly trend of δ^{18}O has been evaluated, and compared with the data of Lanzhou from the database in the global Network of Isotopes in Precipitation (GNIP), as shown in Fig. 2. There is a good consistency between the two groups of data, which show relatively higher values of δ^{18}O in summer, and lower values in winter. The highest values appear from May to September. Since October, the values gradually decreased. Figure 3 shows the local meteoric water lines (LMWL) of the study area. Compared with the global meteoric water lines (GMWL), the slope and intercept of LMWL are relatively lower, indicating a strong evaporation effect (Wu et al. 2010). On the other hand, the slope and intercept of LMWL of Lanzhou are more close to the meteoric water lines in northwest China, which has a slope and an intercept of 7.88 and 9.42 (Liu et al. 1997), respectively.

According to the monthly variation of δ^{18}O values which is compared with the results of GNIP for Lanzhou and the LMWL, it can be verified that the data are collected under a normal year and reliable.

Moisture sources on a large scale

The value of d excess is influenced by many factors (Merlivat and Jouzel 1979; Peng et al. 2005). The initial value is mainly controlled by the relative humidity of the air mass above the water source and has a negative relationship with that parameter (Pfahl and Wernli 2008; Uemura et al. 2008). Therefore, changes of d excess can be a good indicator for meteorological conditions in the water vapor source (Petit et al. 1991). Conversely, with the help of the variations of d excess, it can be an effective way to

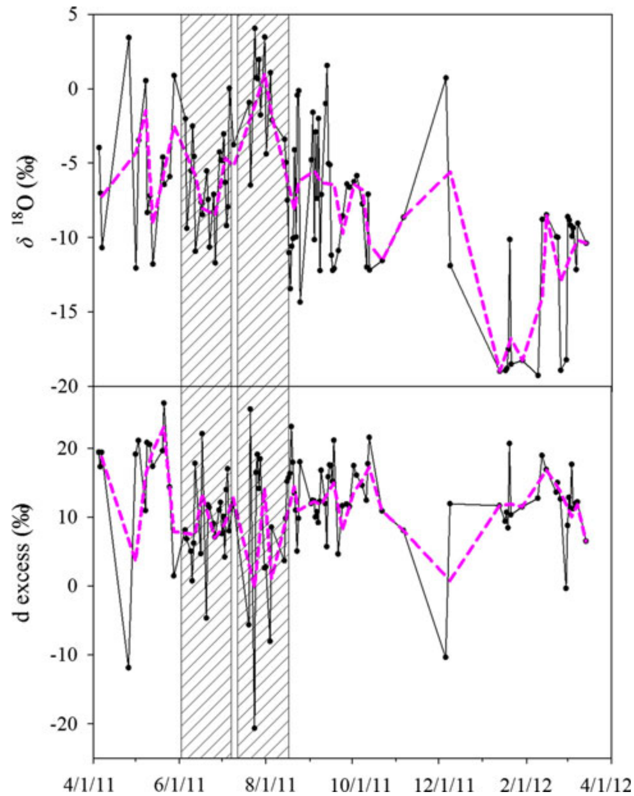

Fig. 2 Monthly variation of δ^{18}O from April 2011 to March 2012. The *circles* refer to the average monthly values of δ^{18}O by the observed samples collected in the four sampling sites. The *triangles* denote the mean δ^{18}O values of Lanzhou using the data from GNIP database of Lanzhou. The two groups of data show a good consistency of variation in a whole year scale

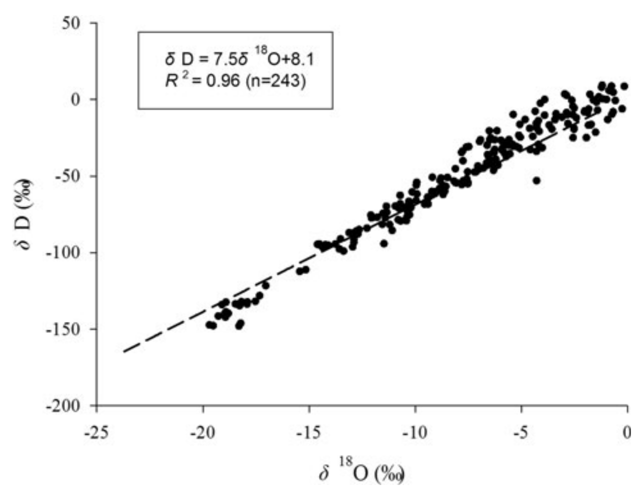

Fig. 3 The local meteoric water lines of Lanzhou by using all the isotopic data collected in four stations from April 2011 to March 2012

trace the moisture sources. In addition, as a result of other factors, d excess will also appear with different patterns of change. Water vapor from land surface, supplying to the air mass, is composed of plant transpiration and evaporation from surface water body (Gat 1996; Gat et al. 1994). The latter one has higher values in d excess. Thus, the d excess in atmospheric water vapor increases when mixed with the recycling moisture. Additionally, secondary evaporation under the cloud base also plays a significant role in affecting the values of d excess. As a result of the preferential evaporation of the light isotopes of ^{1}H and ^{16}O during the secondary evaporation, the heavy isotopes enrich. This causes an increase in the δ values and decrease in the d excess (Peng et al. 2007).

Figure 4 shows the seasonal variations of $\delta^{18}O$ and d excess. The change of $\delta^{18}O$ has an obvious regularity. The values in summer are higher than those in winter, and the "temperature effect" in middle and high latitudes may account for this phenomenon (Dansgaard 1964). The variation of d excess fluctuates on a daily basis, but is relatively stable on a weekly basis which has a mean value of 11.6 ‰. This indicates that the study area is affected by a constant moisture source, which may be the westerly water vapor over a whole year. Moreover, after a comprehensive analysis of $\delta^{18}O$ and d excess in Fig. 4, it can be found that both of $\delta^{18}O$ and d excess decreased from early June to early July, and the lowest values are −11.7 and −4.6 ‰, respectively. The summer monsoon in China generally starts in May and withdraws in late September to October (Wang and Lin 2002). Thus, moisture for precipitation in this period is likely from oceans. The transportation over a long distance may lead to the decreasing of $\delta^{18}O$, according to the "continental effect", and the increase of relative humidity in moisture source should be responsible for the decline of d excess during this period. However, the mode of variation changes from early July to mid-August. The $\delta^{18}O$ values increase significantly while the d excess still declines. The d excess gets much lower than the previous period, the lowest value of which is −20.6 ‰. The enrichment of $\delta^{18}O$ and decreasing of d excess may indicate that there exists a strong evaporation under the cloud base in the region. But, the excessive decline of d excess during this period may also suggest the impact of monsoon moisture. From mid-August to November, the variations of $\delta^{18}O$ and d excess values were relatively stable. After December, $\delta^{18}O$ values began to decrease while the d excess increased. It indicates that the westerly air mass mixed with huge amount of moisture evaporating from the land surface had an effect on this region.

In order to verify the results above, the NOAA Hybrid Single Particle Lagrangian Integrated Trajectory Model (HYSPLIT) 4.9 was applied for simulation, using the NCEP/NCAR global reanalysis from 2011 to 2012. Based

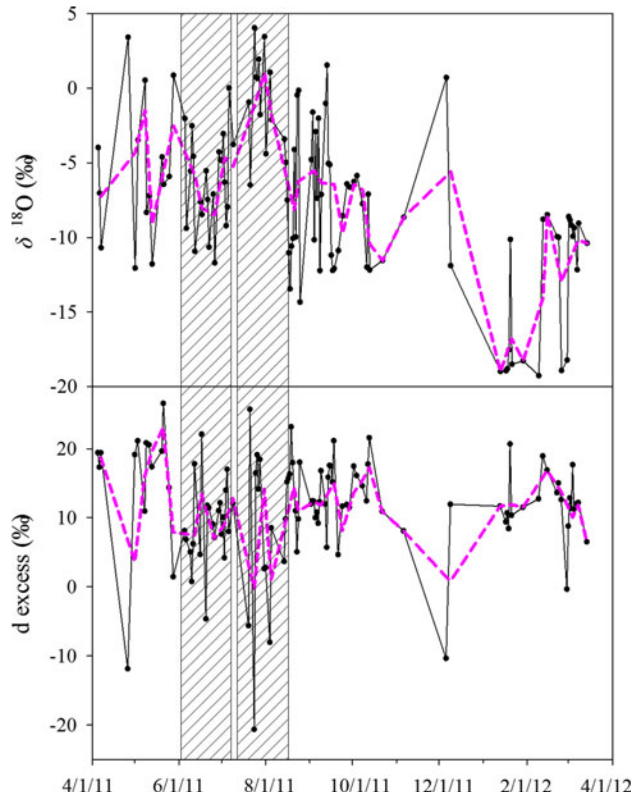

Fig. 4 Seasonal variations of $\delta^{18}O$ and d excess. The *solid lines with circles* refer to the daily variation, and the *dashed lines* show the weekly trend. The *bars* highlight two periods which are from early June to early July and early July to mid-August

on the consistency of precipitation occurring in four stations, 10 periods from 2011 to 2012 were selected. The vapor trajectories have been calculated at 0, 6, 12 and 18 UTC, and each of the trajectories was modeled over a 10-day (240-h) period. Then, the tool of "Trajectory Cluster Analysis" in the software of HYSPLIT 4.9 was used to calculate the average trajectories over the 10 different periods. The result is showing in Fig. 5.

At annual scale, the moisture source influencing the region is mainly the westerly water vapor which originates from the Atlantic Ocean and transports through the arid northwestern China to Lanzhou. Feng et al. (2013) has investigated the moisture sources in Tianshan region and found that the westerly has a dominant effect on northwestern China. However, from early June to early August, the moisture sources affecting the study area change. Not only the westerly vapor affects the study area, but the southeastern moisture also influences it, which corresponds with the decrease of d excess in Fig. 4 in the same period. Moreover, it is not difficult to determine that there still is southeastern moisture from mid-August to mid-October (Fig. 5g–i). If the air mass belongs to the monsoon moisture, then it is contradictory to the fact of the relatively stable changes of d excess in Fig. 4. In this respect, the data

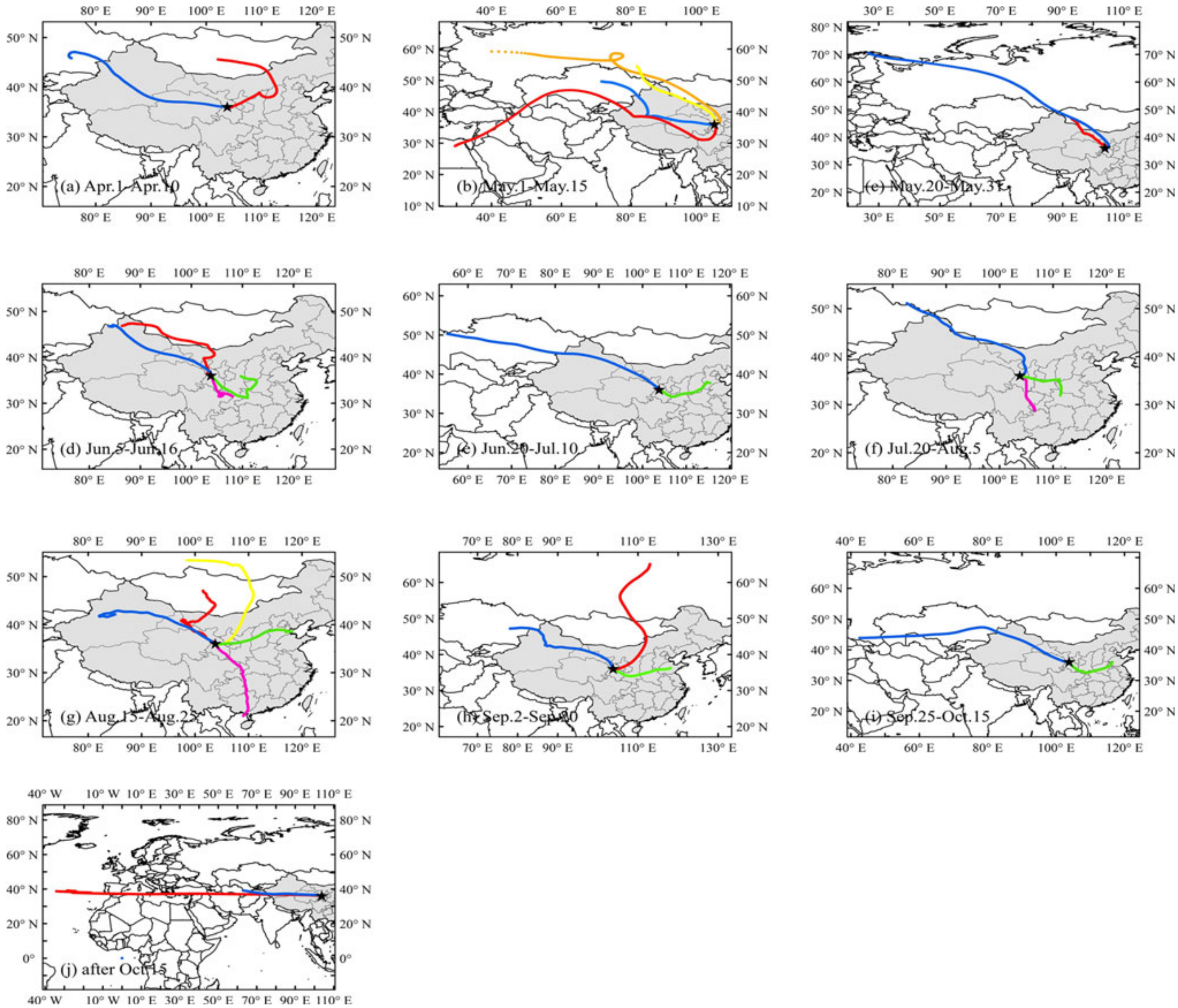

Fig. 5 Modeled trajectory in different periods from 2011 to 2012. **a** From April 1 to 10; **b** from May 1 to 15; **c** from May 20 to 31; **d** from June 5 to 16; **e** from June 20 to July 10; **f** July 20 to August 5; **g** from August 15 to 25; **h** from September 2 to 20; **i** from September 25 to October 15; **j** after October 15

in this period should be further analyzed to confirm the nature of the air mass. After October (Fig. 5j), the vapor source becomes single; the westerly water vapor has a great impact on the region.

In order to make sure whether the study area has been influenced by the monsoon moisture from June to October, the trajectories on rainy days during this period have been calculated by using the HYSPLIT 4.9. The trajectories showing the moisture transport from southeast were chosen and the relative isotopic data were used to calculate the mean value of d excess. The average d excess from some stations in southeastern China was also calculated from June to September for comparison. The d excess in southeastern stations is 9.66 ‰ on average, ranging from 5.3 to 12.45 ‰, as shown in Table 2. The mean d excess in Lanzhou from June to early August is 9.4 ‰, and close to the value of 9.66 ‰. The fact indicates that the region is sure to suffer the monsoon moisture during this period. However, the average d excess from mid-August to early October is 16.3 ‰, and much greater than the average value in southeastern stations. Therefore, it can be inferred that the moisture may be from local evaporation rather than from the monsoon moisture.

The water cycle mechanism on a local scale

According to the research above, the westerly water vapor has a primary impact on this region on a large scale, while in summer, the situation is more complex. On the basis of the "continental effect" (Dansgaard 1964), the isotopic

Table 2 The mean value of d excess in Lanzhou in two periods, and the average d excess from June to September in the stations of southeastern China which are influenced by the Asian summer monsoon

Station	Average d excess (‰)	Period	Data source	Mean value (‰)
Fuzhou	10.44	1985–1992	GNIP	9.67
Hong Kong	8.52	1961–2004	GNIP	
Guilin	12.45	1983–1990	GNIP	
Nanjing	11.11	1987–1992	GNIP	
Xiamen	7.67	2004–2006	Chen et al. 2010	
Guangzhou	12.17	2007–2009	Xie et al. 2011	
Liuzhou	5.3	1988–1992	GNIP	
Lanzhou	9.4	06/05/2011–08/05/2011	This study	12.85
	16.3	08/05/2011–10/05/2011		

Table 3 The $\delta^{18}O$ values of four stations in individual events

Date (mm/dd/yyyy)	$\delta^{18}O$ (‰)				Mode type
	Yongdeng	Lanzhou	Gaolan	Yuzhong	
05/08/2011–05/09/2011	−1.87	−1.46	−4.55	−12.06	Mode 1
05/11/2011	−5.58	−4.30	−6.93	−11.98	
05/28/2011	4.15	4.72	–	−6.27	
06/16/2011–06/17/2011	−2.56	–	−6.14	−11.74	
06/21/2011	−4.59	−5.76	−8.83	−10.63	
06/22/2011	−8.58	−10.49	−10.58	−12.97	
06/25/2011–06/26/2011	−6.43	−10.55	–	−12.87	
06/29/2011	−0.75	−1.35	–	−10.71	
07/04/2011	−4.46	−8.42	−12.64	−11.35	
07/05/2011	−6.59	−6.57	−10.71	–	
07/28/2011	−0.99	−0.97	−3.90	−1.22	
08/01/2011	−4.16	−1.50	–	−7.52	
08/04/2011	0.42	3.354	−0.57	–	
09/06/2011	−1.83	−4.07	−7.75	−15.83	
09/09/2011	−4.14	−0.67	−5.38	−18.29	
09/17/2011	−11.52	−12.23	–	−12.89	
10/11/2011–10/13/2011	−9.03	−6.00	–	−16.30	
Mean value (‰)	−4.03	−4.14	−7.09	−11.51	
Date (mm/dd/yyyy)	$\delta^{18}O$ (‰)				Mode type
	Gaolan	Yongdeng	Lanzhou	Yuzhong	
08/15/2011	−3.36	−7.20	−4.28	−5.04	Mode 2
08/16/2011	−6.50	−8.68	−7.05	−7.74	
08/17/2011	−9.92	−9.19	−10.21	−14.81	
08/18/2011	−9.19	−12.77	−12.94	−18.91	
08/20/2011	−4.82	−11.30	–	−14.08	
08/21/2011	−4.10	−2.52	−5.71	–	
08/22/2011	−5.74	−4.66	–	−19.51	
Mean value (‰)	−6.24	−8.05	−8.04	−13.35	

In mode 1, the values of $\delta^{18}O$ in Yongdeng and Lanzhou station have a similarity to some degree, and the values are greater than the ones in Ganlan and Yuzhong. In mode 2, $\delta^{18}O$ values in Gaolan become the highest data were analyzed to discuss the water cycle mechanism on a local scale, as shown in Table 3.

There appear two modes of moving patterns of moisture (Fig. 6). In mode 1, the values in Lanzhou and Yongdeng are higher. The mean values of both are −4.14 and −4.3 ‰, respectively. In addition, the $\delta^{18}O$ values of the two stations in individual precipitation event have some similarities. The $\delta^{18}O$ gets lower in Gaolan, and it depletes to the lowest value in Yuzhong station with an average of −11.51 ‰. Therefore, it can be inferred that the moisture, taken by the westerlies, may firstly go across from Lanzhou and Yongdeng, and then to the stations of Gaolan and Yuzhong. In mode 2, the value of $\delta^{18}O$ in Gaolan, with an average of −6.24 ‰, becomes the highest, while the remaining three stations are significantly lower. Moreover, mode 2 is mainly concentrated after mid-August, and it corresponds with the eastern moisture source in Fig. 5g. Thus, it can be inferred that the water vapor may transport from Gaolan to Lanzhou, Yuzhong and Yongdeng, respectively.

The contribution rate of moisture from land surface

The contribution rate of moisture evaporated from land surface has been calculated by using a relative model. Recently, many researchers have used the approach to calculate the contribution rate in different areas, and got better results (Peng et al. 2010; Xu et al. 2011; Froehlich et al. 2008). From the research above, the westerlies is the main water vapor source affecting the region on a large scale. Thus, the westerly water vapor has been regarded as the primary input factor. The moisture-recycling fraction can be evaluated by the following equation (Peng et al. 2005):

$$R = \frac{(d_{\mathrm{loc}} - d_{\mathrm{air}})}{(d_{\mathrm{vap}} - d_{\mathrm{air}})} \quad (1)$$

In Eq. (1), d_{loc} is the d excess of precipitation collected in sampling sites, d_{air} refer to the d excess of westerly air mass, d_{vap} is the d excess of water vapor originated from land surface. In Eq. (1), the d_{air} is assumed to be the mean value of d excess of Yongdeng (Peng et al. 2010). The d excess of d_{vap} should be further estimated from the Craig-Gordon equation (Gat et al. 1994; Craig and Gordon 1965).

$$\delta_{\mathrm{vap}} = \frac{(\delta_{\mathrm{sw}} - h\delta_{\mathrm{atm}} - \varepsilon)}{(1-h)} \quad (2)$$

In Eq. (2), δ_{sw} is the isotopic value of the surface water. According to Peng et al. (2005), the value of δ_{sw} can be replaced by the long-term average of annual weighted mean isotope composition of precipitation, δ_{atm} is the isotopic value of the atmospheric moisture, h is relative humidity and ε stands for a combination of both equilibrium and kinetic enrichment factors (Peng et al. 2010).

The contribution rate of Lanzhou and surrounding areas ranges between 2.0 and 6.3 %, and is 3.6 % on average. Gat et al. (1994) studied the Great Lakes and found that the moisture-recycling fraction only ranges between 4.6 and 15.7 % although the area has abundant water resources in land. Moreover, Froehlich et al. (2008) calculated the rate on the main ridge of the Austrian Alps and also got a small value, which is from 2.5 to 3 %. Therefore, combined with the actual situations of Lanzhou which is located in an arid and semi-arid region, we infer that the lack of water body in land surface may be an important reason which leads to the small contribution rate.

Existence of evaporation effect

The effect of secondary evaporation means the evaporation of rain falling from the cloud base to the ground. The rainfall influenced by the evaporation effect shows the characteristics of an enrichment of $\delta^{18}O$ and decline of d excess (Liu et al. 2008). Based on the theory, we calculated the mean values of $\delta^{18}O$ and d excess, choosing the isotopic data which simultaneously corresponds to the two conditions above to analyze. Figure 7 shows the

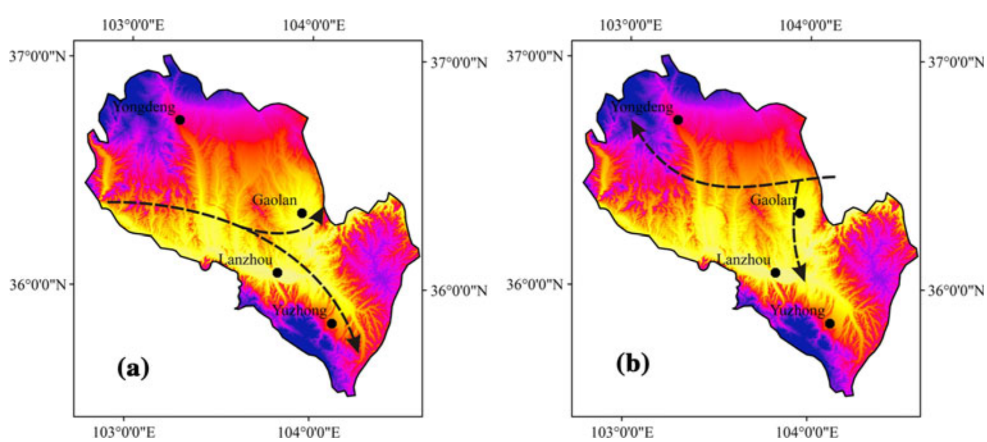

Fig. 6 The water cycle mechanism on a local scale. The *dashed lines* refer to the trajectories of moisture influencing the region. *Solid circles* are sampling sites. In **a** the trajectory is from Lanzhou, Yongdeng to Gaolan and Yuzhong, and in **b** the trajectory is along Gaolan to Yongdeng, Lanzhou and Yuzhong

evaporation effect in the region. The effect is mainly concentrated from June to September in summer. However, after October, the effect gradually decreases.

Factors influencing the evaporation effect

In addition to the characteristic of the enrichment of $\delta^{18}O$ and decrease of d excess, the rain samples affected by evaporation effect also have another feature. That is the decline of the slopes of meteoric water lines as a result of the kinetic isotope effects (Peng et al. 2007). Thus, with the help of two indices of slope and d excess, the evaporation under the cloud base can be effectively discussed. Air temperature, relative humidity and precipitation amounts are the main factors influencing the evaporation (Liu et al. 2008); therefore, the three meteorological parameters above were chosen to investigate the secondary effect in the area.

As shown in Table 4, relative humidity has an obvious impact on sub-cloud evaporation. Along with the decline of relative humidity, both slope and d excess decreases gradually. The amplitude is apparent, and the slope decreases from 8.05, which is close to 8 in GMWL, to 6.7. d Excess dropped from 15.2 to 3.1 ‰. All of the data above indicate that the evaporation effect is gradually increasing in the region. Under the impact of temperature, there also emerges a similar trend of variation. With the increasing of temperature, both of slope and d excess decrease except the data below 0 °C which are mainly snow samples. However, when the factor of precipitation amount is considered, the variations of slope and d excess are different. The slope and d excess strangely increase when the rainfall amount is between 0 and 10 mm. Until the precipitation amount is

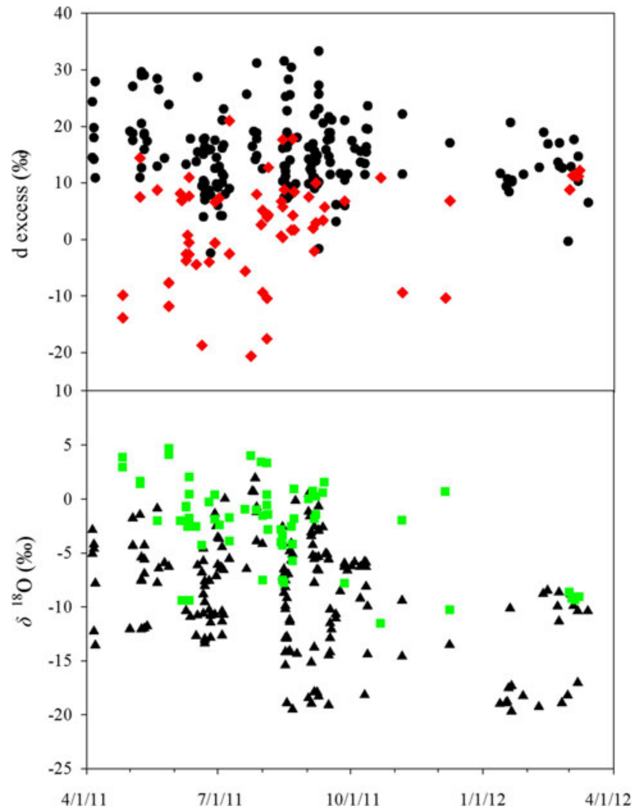

Fig. 7 The existence of secondary evaporation. The mean values of d excess and $\delta^{18}O$ have been calculated by using the entire observed data. The data which simultaneously conform to the following two conditions have been chosen as the samples which experienced secondary evaporation. (1) The d excess is lower than the average value. (2) Their $\delta^{18}O$ values are greater than the mean value. The *red diamonds* refer to the observed d excess lower than the average value, and the *solid circles* are the d excess greater than the average. The *green squares* show the $\delta^{18}O$ values greater than the average and the *solid triangles* mean the $\delta^{18}O$ values lower than the mean value

Table 4 The effect of secondary evaporation influenced by precipitation, temperature and relative humidity

Meteorological parameters	Data range	Slope	Coefficient of correlation	d excess (‰)	Number of samples
Relative humidity (%)	90–100	8.05	0.97	15.2	26
	80–90	8.07	0.97	13.3	89
	70–80	7.4	0.95	11.7	46
	60–70	6.8	0.88	8.8	19
	<60	6.7	0.86	3.1	25
Temperature (°C)	<0	7.6	0.97	12.1	21
	0–10	7.8	0.94	18.1	43
	10–15	7.6	0.97	11.1	58
	15–20	7.3	0.95	11.2	92
	20–30	7.2	0.89	6.9	19
Precipitation amount (mm)	0–2	7.3	0.95	10.8	137
	2–5	7.8	0.95	12.7	48
	5–10	7.9	0.96	15.8	28
	10–15	7.8	0.98	14.4	8
	15–20	7.7	0.98	13.9	5

Table 5 Secondary evaporation affected by temperature and relative humidity during the rainfall amount of 0–10 mm

Temperature (°C)	Slope	Coefficient of correlation	d excess (‰)	Relative humidity (%)	Slope	Coefficient of correlation	d excess (‰)
<0	7.6	0.97	12.05	90–100	8.1	0.98	15.9
0–10	8	0.96	18.5	80–90	8.1	0.97	13.1
10–20	7.4	0.95	10.4	70–80	7.4	0.95	12.5
20–30	6.7	0.73	5.9	60–70	6.8	0.88	8.8
				<60	6.7	0.83	2.5

>10 mm, the two indices begin to decrease. Thus, the inferred precipitation amounts may not influence the evaporation effect during the 0–10 mm rainfall amount; or, in other words, the evaporation effect may be covered by other indices in that amount range.

In order to further investigate the secondary evaporation effect during the rainfall amount of 0–10 mm, the relative isotopic data during that scope were extracted for discussion. Temperature and relative humidity factors are considered as the main factors in this process (Table 5). The result shows that during the 0–10 mm precipitation amount, both of d excess and slope decrease significantly when we regard temperature and relative humidity as the main factors. Therefore, it is not difficult to conclude the factors of temperature and relative humidity have a great impact on the evaporation effect, while the influence of precipitation does not appear in that scope.

Conclusions

By using 243 event-based precipitation samples, the variations of moisture sources in different scales and secondary evaporation in Lanzhou and surrounding areas have been discussed. Conclusions reached are:

(1) On a large scale, Lanzhou is mainly influenced by the westerly water vapor over a whole year. Except the westerlies, monsoon moisture has an impact on the study area during the period from June to early August. On a local scale, the inferred trajectory of moisture appears in two modes, which is from Lanzhou and Yongdeng to Yuzhong and Gaolan, and from Gaolan to Lanzhou, Yuzhong and Yongdeng. In addition, the contribution rate of recycling moisture is 3.6 % on average. The lack of surface water source may be responsible for the relatively low value.

(2) There exists secondary evaporation in the region. Temperature, relative humidity and precipitation amounts are the main factors influencing evaporation below the cloud base. The impact of precipitation is not shown during the rainfall amount of 0–10 mm. However, temperature and relative humidity have a great impact on evaporation in that rainfall scope.

Acknowledgments The study is financially supported by the National Natural Science Foundation of China (No. 41161012; No. 41240001), the National Basic Research Program of China (973 Program) (No. 2013CBA01801) and the Basic Scientific Research Foundation in University of Gansu Province. The authors thank David Clements for revising the original manuscript, and the workers in the national meteorological stations of Yuzhong, Yongdeng and Gaolan for collecting the samples.

References

Carroll M, Romanek C, Paddock L (2006) The relationship between the hydrogen and oxygen isotopes of freshwater bivalve shells and their home streams. Chem Geol 234(3–4):211–222

Chen JF, Cao JP, Huang YP (2010) The hydrogen and oxygen isotope composition of precipitation in the Xiamen coastal area. J Mar Sci 28(1):11–17 (in Chinese with English abstracts)

Craig H, Gordon LI (1965) Deuterium and oxygen-18 variations in the ocean and the marine atmosphere. In: Tongiorgi E (ed) Proceedings of the Conference on Stable Isotopes in Oceanographic Studies and Paleotemperatures. Laboratory of Geology and Nuclear Science, Pisa, pp 9–130

Criss RE (1999) Principles of stable isotope distribution. Oxford University Press, New York, pp 89–136

Dansgaard W (1964) Stable isotope in precipitation. Tellus 16(4):436–468

Feng F, Li ZQ, Zhang MJ, Jin S, Dong ZW (2013) Deuterium and oxygen 18 in precipitation and atmospheric moisture in the upper Urumqi River Basin, eastern Tianshan Mountains. Environ Earth Sci 68(4):1199–1209

Froehlich K, Kralik M, Papesch W, Rank D, Scheifinger H, Stichler W (2008) Deuterium excess in precipitation of Alpine regions—moisture recycling. Isotopes Environ Health Stud 44(1):61–70

Gat JR (1996) Oxygen and hydrogen isotopes in the hydrologic cycle. Annu Rev Earth Pl Sc 24:225–262

Gat JR, Matsui E (1991) Atmospheric water balance in the Amazon Basin: an isotopic evapo-transpiration model. J Geophys Res 96(D7):13179–13188

Gat JR, Bowser CJ, Kendall C (1994) The contribution of evaporation from the Great Lakes to the continental atmosphere, estimate based on stable isotope data. Geophys Res Lett 21(7):557–560

Kress A, Saurer M, Siegwolf RTW, Frank DC, Esper J, Bugmann H (2010) A 350 years drought reconstruction from Alpine tree ring stable isotopes. Glob Biogeochem Cycle 24:GB2011. doi:10.1029/2009GB003613

Kumar US, Kumar B, Rai SP, Sharma S (2010) Stable isotope ratios in precipitation and their relationship with meteorological

conditions in the Kumaon Himalayas, India. J Hydrol 391(1–2):1–8
Lachniet MS (2008) Climatic and environmental controls on speleothem oxygen isotopes values. Quat Sci Rev 28(5–6):412–432
Li JJ, Feng ZD, Tang LY (1988) Late quaternary monsoon patterns on the loess plateau of China. Earth Surf Proc Land 13(2):125–135
Liu JD, Zhao YC, Liu EK, Wang DS (1997) Discussion on the stable isotope time-space distribution law of China atmospheric precipitation. Sci Technol Reconnaiss 3:34–39 (in Chinese with English abstracts)
Liu ZF, Tian LD, Yao TD, Yu WS (2008) Seasonal deuterium excess in Nagqu precipitation: influence of moisture transport and recycling in the middle of Tibetan Plateau. Environ Geol 55(7):1501–1506
Merlivat L, Jouzel J (1979) Global climate interpretation of the deuterium-oxygen18 relationship for precipitation. J Geophys Res 84(C8):5029–5033
Pang ZH, Kong YL, Froehlich K, Huang TM, Yuan LJ, Li ZQ, Wang FT (2011) Processes affecting isotopes in precipitation of an arid region. Tellus 63(3):352–359
Peng H, Mayer B, Norman A, Roy H (2005) Modeling of hydrogen and oxygen isotope compositions for local precipitation. Tellus 57(4):273–282
Peng H, Mayer B, Harris S, Krouse HR (2007) The influence of below-cloud secondary effects on the stable isotope composition of hydrogen and oxygen in precipitation at Calgary, Alberta, Canada. Tellus 59(4):698–704
Peng TR, Wang CH, Huang CC, Fei LY, Chen CA, Hwong JL (2010) Stable isotopic characteristic of Taiwan's precipitation: a case study of western Pacific monsoon region. Earth Planet Sci Lett 289(3–4):357–366
Petit JR, White JWC, Young NW, Jouzel J, Korotkevich YS (1991) Deuterium excess in recent antarctic snow. J Geophys Res 96(D3):5113–5122
Pfahl S, Wernli H (2008) Air parcel trajectory analysis of stable isotopes in water vapor in the eastern Mediterranean. J Geophys Res 113(D20):D20104. doi:10.1029/2008JD009839
Qian WH, Lin X, Zhu YF, Xu Y, Fu JL (2007) Climatic regime shift and decadal anomalous events in China. Clim Chang 84(2):167–189
Qian WH, Ding T, Hu HR, Lin X, Qin AM (2009) An overview of dry-wet climate variability among monsoon-westerly regions and the monsoon northernmost marginal active zone in China. Adv Atmos Sci 26(4):630–641
Sengupta S, Sarkar A (2006) Stable isotope evidence of dual (Arabian Sea and Bay of Bengal) vapour sources in monsoonal precipitation over north India. Earth Planet Sc Lett 250(3–4):511–521
Steen-Larsen HC, Masson-Delmotte V, Sjolte J, Johnsen SJ, Vinther BM, Bréon FM, Clausen HB, Dahl-Jensen D, Falourd S, Fettweis X, Gallée H, Jouzel J, Kageyama M, Lerche H, Minster B, Picard G, Punge HJ, Risi C, Salas D, Schwander J, Steffen K, Sveinbjörnsdóttir AE, Svensson A, White J (2011) Understanding the climatic signal in the water stable isotope records from the NEEM shallow firn/ice cores in northwest Greenland. J Geophys Res 116:D06108. doi:10.1029/2010JD014311
Tian LD, Yao TD, Macclune K, White JWC, Schilla A, Vaughn B, Vachon R, Ichiyanagi K (2007) Stable isotopic variations in west China: a consideration of moisture sources. J Geophys Res 112:D10112. doi:10.1029/2006JD007718
Uemura R, Matsui Y, Yoshimura K, Motoyama H, Yoshida N (2008) Evidence of deuterium excess in water vapor as an indicator of ocean surface conditions. J Geophys Res 113(D19):D19114. doi:10.1029/2008JD010209
Vodila G, Palcsu L, Futo I, Szántó Z (2011) A 9-year record of stable isotope ratios of precipitation in Eastern Hungary: implications on isotope hydrology and regional palaeoclimatology. J Hydrol 400(1–2):144–153
Wang B, Lin H (2002) Rainy season of the Asian-Pacific summer monsoon. J Clim 15:386–398
West AG, Golds GR, Brooks PD, Dawson TE (2010) Discrepancies between isotope ratio infrared spectroscopy and isotope ratio mass spectrometry for the stable isotope analysis of plant and soil waters. Rapid Commun Mass Sp 24(14):1948–1954
Wu JK, Ding Y, Ye B, Yang Q, Zhang X, Wang J (2010) Spatio-temporal variation of stable isotopes in precipitation in the Heihe River Basin, Northwestern China. Environ Earth Sci 61(6):1123–1134
Xie LH, Wei GJ, Deng WF, Zhao XL (2011) Daily $\delta^{18}O$ and δD of precipitations from 2007 to 2009 in Guangzhou, South China: implications for changes of moisture sources. J Hydrol 400(3–4):477–489
Xu YW, Kang SC, Zhang YL, Zhang YJ (2011) A method for estimating the contribution of evaporative vapor from Nam Co to local atmospheric vapor based on stable isotopes of water bodies. Chin Sci Bull 56(14):1511–1517
Yamanaka T, Tsujimura M, Oyunbaatar D, Davaa G (2007) Isotopic variation of precipitation over eastern Mongolia and its implication for the atmospheric water cycle. J Hydrol 333(1):21–34
Zhao LJ, Yin L, Xiao HL, Cheng GD, Zhou MX, Yang YG, Li CZ, Zhou J (2011) Isotopic evidence for the moisture origin and composition of surface runoff in the headwaters of the Heihe River basin. Chin Sci Bull 56(4–5). doi:10.1007/s11434-010-4278-x